Electronic Supplementary Material (ESI) for Nanoscale.

Supporting Information

Plasmonic near-touching titanium oxide nanoparticles to realize solar energy harvesting and effective local heating

Jiahao Yan, Pu Liu, Churong Ma, Zhaoyong Lin, & Guowei Yang

State Key Laboratory of Optoelectronic Materials and Technologies, Nanotechnology Research Center, School of Materials Science & Engineering, School of Physics & Engineering, Sun Yat-sen University, Guangzhou 510275, Guangdong, P. R. China.

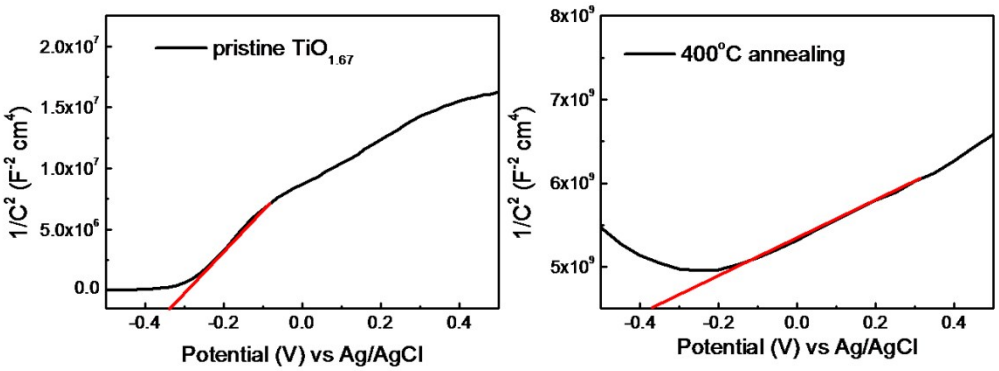

Figure S1. Mott-Schottky plots of pristine $TiO_{1.67}$ sample (left) and the sample after 400°C annealing (right).

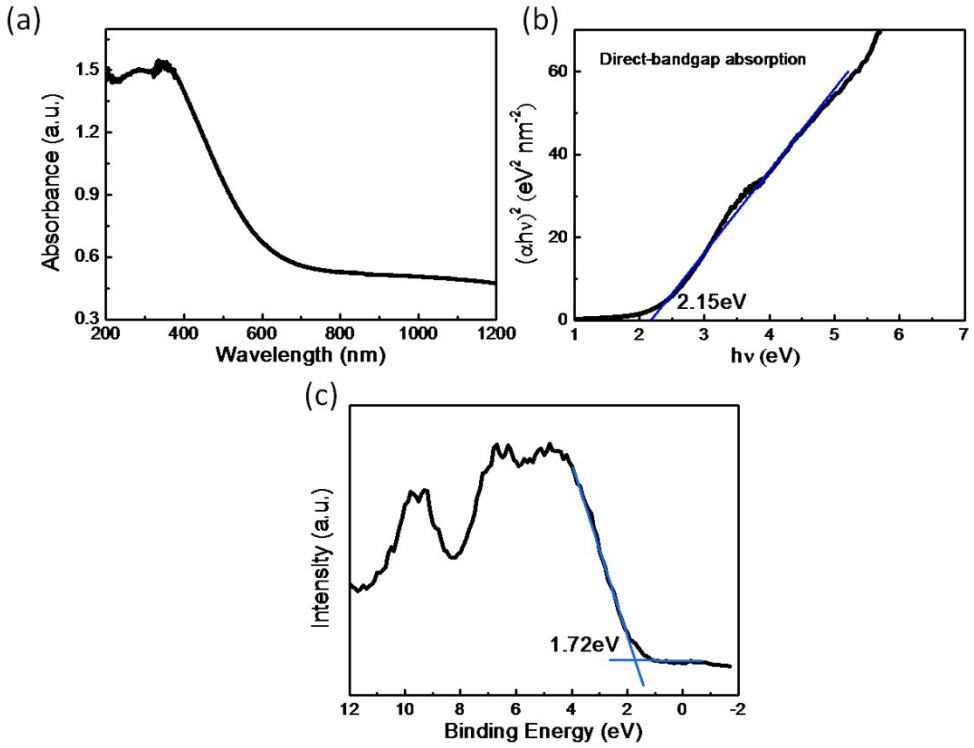

Figure S2. (a)Absorbance of $TiO_{1.67}$ colloidal suspension. (b) The typical Tauc plot derived from the UV-vis absorption spectrum. (c) Valence-band XPS spectra of $TiO_{1.67}$ NPs.

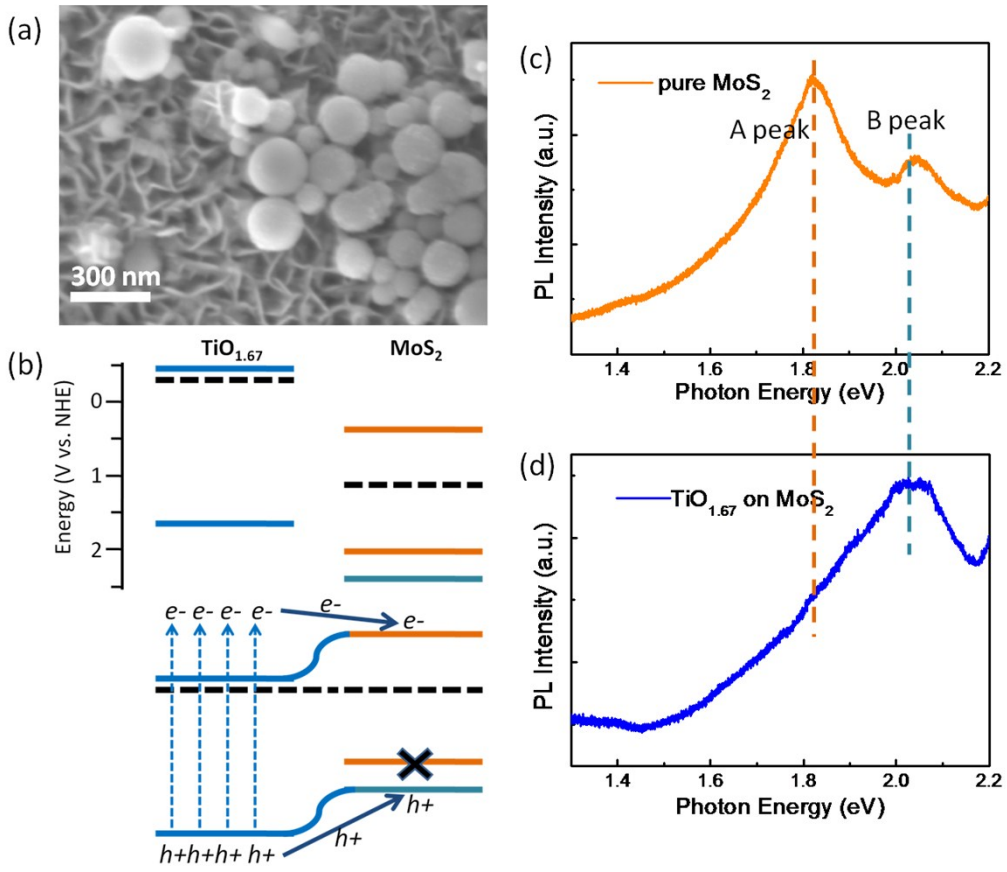

Figure S3. MoS2 PL manipulation by interband plasmon resonance in $TiO_{1.67}$ NPs. (a) SEM images showing $TiO_{1.67}$ NPs loaded on few-layer MoS_2 flakes. (b) The energy levels of $TiO_{1.67}$, MoS2 and the formed p-n junction when combining together. Arrows show the injection direction of hot carriers. And the orange line in the VB of MoS_2 means A band, while the green line means B band. (c) PL spectrum of pure MoS_2 layer. (d) PL spectrum of $TiO_{1.67}$ loaded MoS_2 layer.

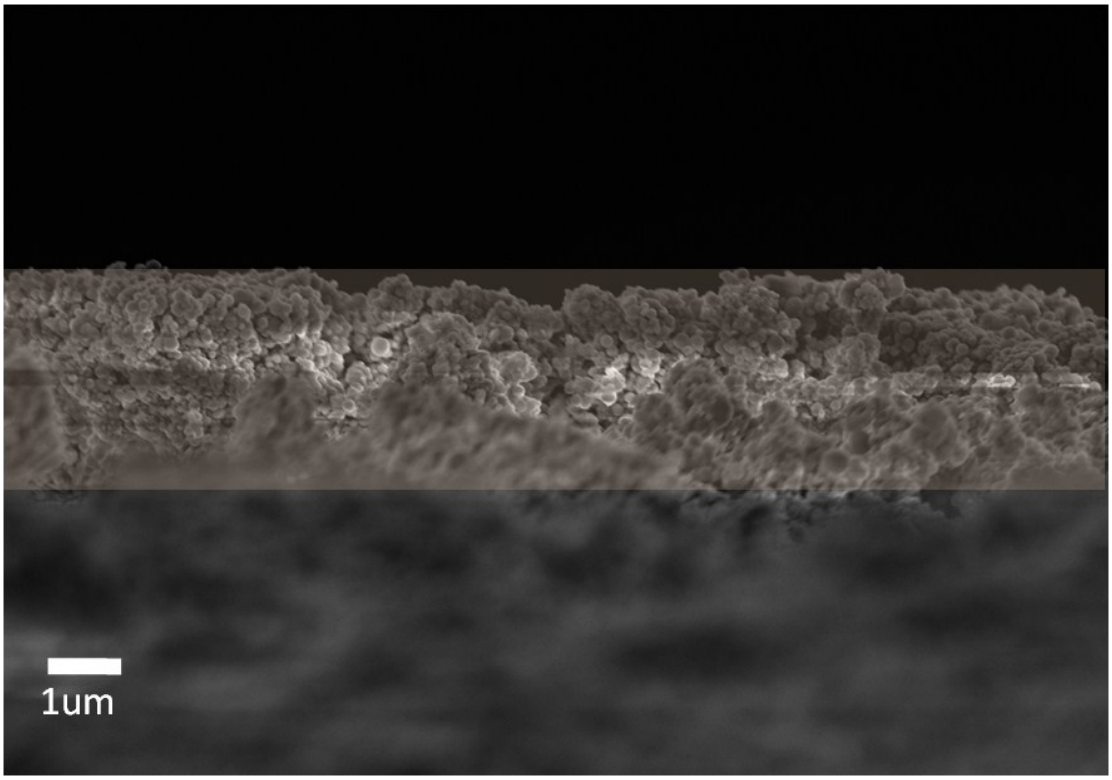

Figure S4. The cross-sectional SEM image of $TiO_{1.67}$ NPs layer marked by the rectangular region.

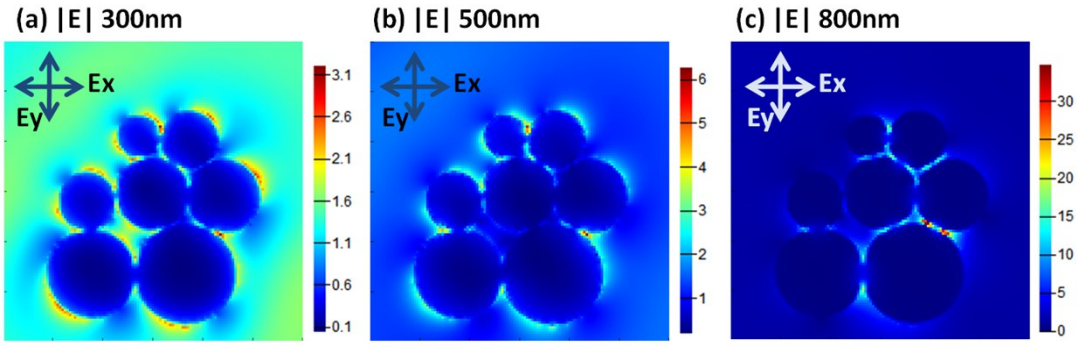

Figure S5. Electric field distributions of Au NPs heptamer (the diameters are 95, 105, 105, 115, 115, 175 and 200 nm) at $\lambda = 300nm$ (a), $\lambda = 500nm$ (b) and $\lambda = 800nm$ (c).

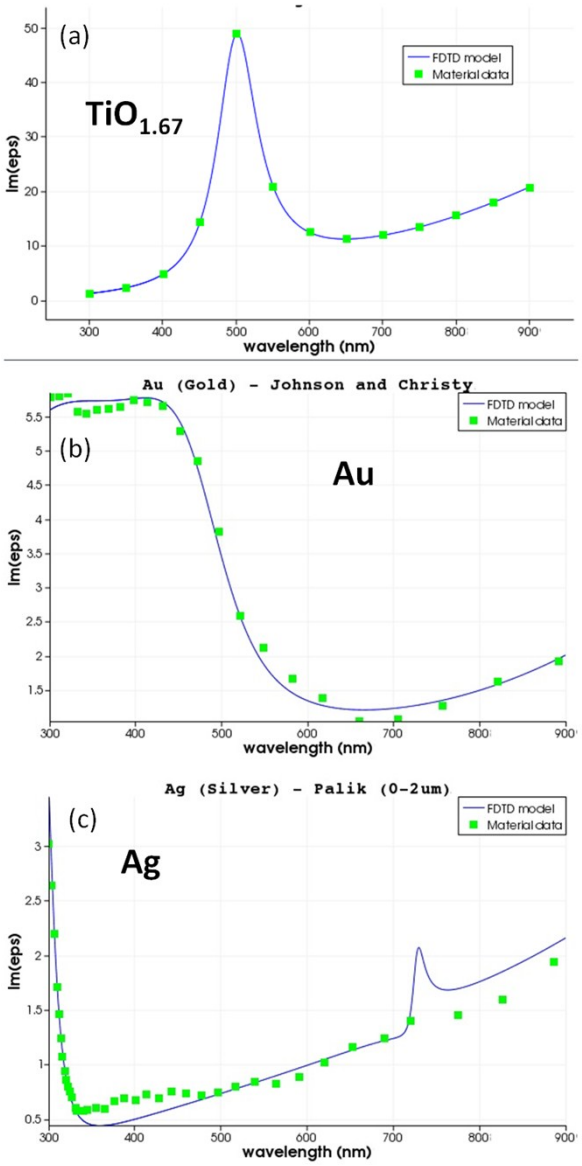

Figure S6. Comparison among $TiO_{1.67}$, Au and Ag. (a) The calculated imaginary part of $TiO_{1.67}$'s dielectric function (dotted line) and the fitted curve by FDTD. (b and c) The imaginary parts of the dielectric function of Au and Ag from references (dotted line) and the fitted curves by FDTD.

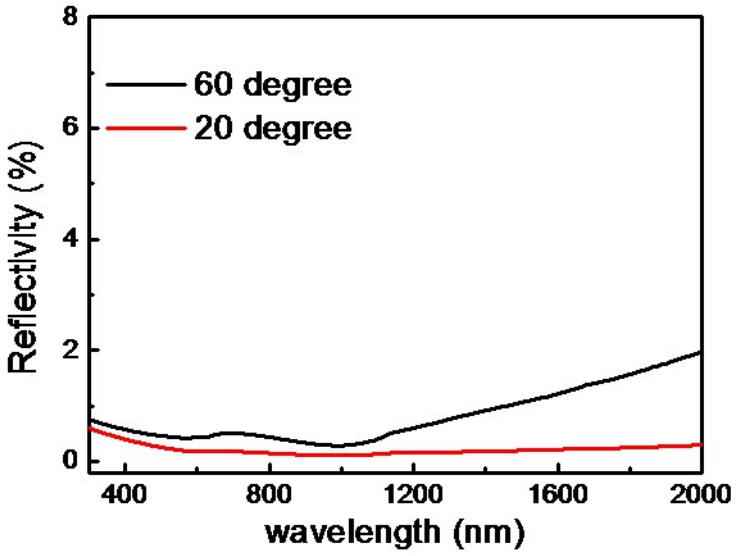

Figure S7. The specular reflectance spectra under different incident angles: 20^{o} (red curve) and 60^{o} (black curve). The optical signals were detected at -20^{o} and -60^{o} respectively.

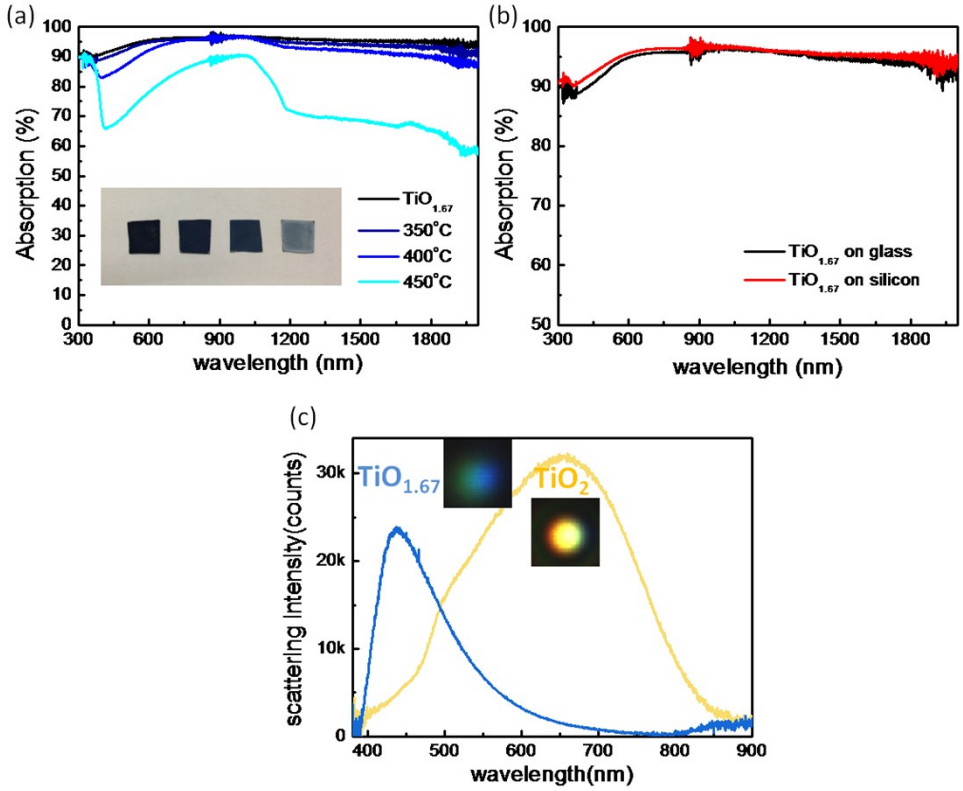

Figure S8. Optical properties of titanium oxide with different carrier densities. (a) Absorption spectra of NPs layer after annealing under different temperature. Inset: From left to right, original $TiO_{1.67}$ absorber and the absorbers annealed under 350°C, 400°C and 450°C. (b) Absorption spectra of $TiO_{1.67}$ NPs layer on silicon(red curve) and glass (black curve). (c)Scattering spectra of $TiO_{1.67}$ NP and TiO_2 NP with the same diameter.

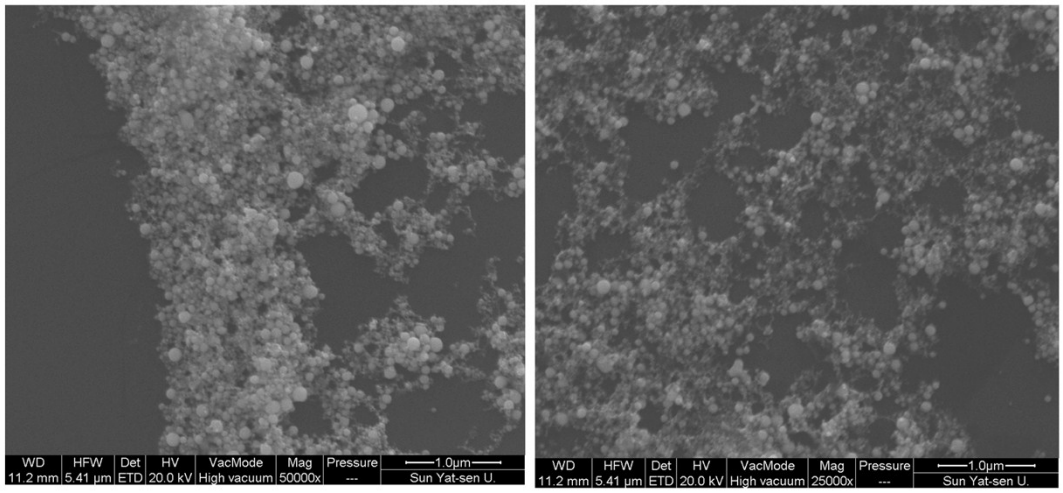

Figure S9. SEM images showing the morphology and size distribution of Au NPs fabricated via fs-LAL.